Metabolic signature of the aging eye in mice

Yekai Wang[1,2], **Allison Grenell**[1,2], **Fanyi Zhong**[3], **Michelle Yam**[1,2], **Allison Hauer**[1,2], **Elizabeth Gregor**[1,2], **Siyan Zhu**[1,2], **Daniel Lohner**[1,2], **Jiangjiang Zhu**[3], and **Jianhai Du**[1,2,*]

[1]Department of Ophthalmology, West Virginia University, Morgantown, WV 26506

[2]Department of Biochemistry, West Virginia University, Morgantown, WV 26506

[3]Department of Chemistry & Biochemistry, Miami University, Oxford, OH, 45056, USA.

Abstract

Aging is a major risk factor for age-related ocular diseases including age-related macular degeneration (AMD) in the retina and retinal pigment epithelium (RPE), cataracts in the lens, glaucoma in the optic nerve, and dry eye syndrome in the cornea. We used targeted-metabolomics to analyze metabolites from young (6 weeks) and old (73 weeks) eyes in C57 BL6/J mice. Old mice had diminished electroretinogram responses and decreased number of photoreceptors in their retinas. Among the 297 detected metabolites, 45–114 metabolites are significantly altered in aged eye tissues, mostly in the neuronal tissues (retina and optic nerve) and less in cornea, RPE/choroid and lens. We noted that changes of metabolites in mitochondrial metabolism and glucose metabolism are common features in the aged retina, RPE/choroid and optic nerve. The aging retina, cornea and optic nerve also share similar changes in NAD, 1- methylnicotinamides, 3- methylhistidine and other methylated metabolites. Metabolites in taurine metabolism are strikingly influenced by aging in the cornea and lens. In conclusion, the aging eye has both common and tissue-specific metabolic signatures. These changes may be attributed to dysregulated mitochondrial metabolism, re-programed glucose metabolism and impaired methylation in the aging eye. Our findings provide biochemical insights into the mechanisms of age-related ocular changes.

Keywords

Metabolite; aging; retina; RPE; lens; cornea; optic nerve

1. Introduction

As we age, the eye undergoes a gradual decline of visual function. This age-related visual deterioration is a combination of structural changes in the ocular tissues including the cornea, lens, retina, retinal pigment epithelium (RPE), choroid and optic nerve. With aging, the number of corneal endothelial cells declines and the epithelium-derived glands including the lacrimal and meibomian glands decrease their production of tears to lubricate the cornea (Gambato et al., 2015; Gipson, 2013; Mustonen et al., 1998). The aging lens decreases its ability to change shape (presbyopia), which is most likely attributed to modifications in the cortical fibre cells (Duncan et al., 1997; Salvi et al., 2006). The populations of neurons in the retina decrease with loss of visual acuity and sensitivity (Lei et al., 2011; Nadal-Nicolas et al., 2018). The microcirculation in the macula, the cone photoreceptor-enriched central region of the retina also declines with age (Salvi et al., 2006). RPE loses melanin and lipofuscin deposits accumulate in the RPE (Delori et al., 2001; Sarna et al., 2003). Aged Bruch's membrane, the innermost layer of the choroid, becomes thickened and basal laminar and basal linear deposits accumulate (Johnson et al., 2007; Li et al., 2005). There also is an age-related decrease in the number of optic nerve axons and an increase in elastic fibres (Cavallotti et al., 2003; Salvi et al., 2006).

Aging is associated with many ocular diseases including Fuch's dystrophy, dry eye syndrome, cataracts, presbyopia, age-related macular degeneration (AMD), diabetic retinopathy and glaucoma. These diseases cause visual impairment in 4–20% of adults over the age of 65 (Chader and Taylor, 2013; Delcourt et al., 2010; Lin et al., 2016; Whitcomb et al., 2013). Poor visual function significantly reduces quality of life and is a strong predictor of mortality (Lott et al., 2010). However, the biochemical basis of aging and age- related eye diseases has not been determined. Understanding how aging influences the eye should yield valuable information for both basic and clinical applications.

Metabolic change is intimately entangled with aging and age-related disease at the molecular and cellular levels (Dhillon and Denu, 2017; Feng et al., 2016). Mitochondrial dysfunction including decreased energy metabolism and impaired antioxidant defenses has been reported in aging lens epithelial cells, retina, RPE and optic nerve (Ferrington et al., 2017; He et al., 2010; He and Tombran-Tink, 2010; Kubota et al., 2016; Lee et al., 2016; Lopez Sanchez et al., 2016; Maresca et al., 2013; Rohrer et al., 2016; Stahon et al., 2016). Improving mitochondrial metabolism can attenuate age-related visual decline in animal models (Mills et al., 2016; Weinrich et al., 2017). A recent study reported that supplementation with an NAD precursor could prevent glaucoma in aged mice by modulating mitochondrial dysfunction (Williams et al., 2017). Identifying metabolic changes that occur in the aging eye is critical for understanding the aging process and for identifying novel targets for disease treatment.

Steady state metabolite concentrations reflect the status of metabolism. Mass spectrometry (MS) coupled with liquid chromatography (LC) or gas chromatography (GC), provides a sensitive and high- throughput platform to measure hundreds of metabolites in a single analysis (Cajka and Fiehn, 2016). In this study, we used targeted metabolomics to evaluate 297 metabolites in young and old ocular tissues including cornea, lens, retina, RPE/choroid,

and optic nerve from C57BL/6J mice. Mice are not an ideal model for AMD as they do not have an anatomical macula. Nevertheless, the mouse is the most widely used animal model for research in eye diseases because of the availability of genetic mutants, its capability of recapitulating key pathological processes in human eye diseases and its cost-effectiveness (Elizabeth Rakoczy et al., 2006; Pennesi et al., 2012; Zeiss, 2010). We have found that mitochondrial metabolism-related metabolites and some methylated metabolites are altered in almost all the aging tissues, suggesting a common feature for the aging eye. Additionally, we identified tissue-specific age- related metabolic changes. This study is the first comprehensive comparison of metabolites in young and old ocular tissues from mice.

2. Materials and methods

2.1. Animals

C57 BL/6J mice of both sexes at 6 weeks were used for the young group and 73 weeks for the aged group. Both the young and aged mice were purchased from Jackson Lab. Mouse experiments were performed in accordance with the National Institutes of Health guidelines and the protocol approved by Institutional Animal Care and Use Committee of West Virginia University.

2.2. Electroretinogram (ERG)

ERGs were performed using the UTAS Visual Diagnostic System with BigShot Ganzfeld with UBA- 4200 amplifier and interface, and EMWIN 9.0.0 software (LKC Technologies, Gaithersburg, MD, USA). Mice were dark adapted overnight. All preparations were done under red light. Eyes were dilated using a 1:1 mixture of 2.5 % phenylephrine (Paragon) and 1% tropicamide (Sandoz). Mice were sedated (1.5% isoflurane with 2.5 l/min (lpm) oxygen flow rate, 40°C) with an induction chamber (N=10 from five animals). After ten minutes of dilation, animals were placed on a heated platform (40°C) where they continued to receive a constant flow of isoflurane from a nose cone. A reference electrode was placed subcutaneously in the back of the neck (LKC Technologies, #95–016.) Electrodes made from 0.125 mm silver wire were carefully positioned closely above the cornea with contact being made by GenTeal Tears Lubricant Eye gel (Alcon). In darkness, scotopic recordings were elicited using flashes of LED white light at increasing flash intensities (−32, −24, −12, −4, 0 dB) responses were averaged at each light intensity. Immediately after scotopic recordings, animals were light adapted for 10 minutes to white background light (30 cds/ m^2.) To keep eyes moist, Systane Ultra Lubricant Eye Drops (Alcon) were applied periodically. With continuous background light, photopic response was elicited with increasing flash intensities (0, 3, 5, 10, 15, 25 dB) again, with LED white light. During data analysis, values were normalized to the baseline and each eye was evaluated separately to determine the A-wave and B-wave amplitudes. Amplitudes were averaged together and graphed.

2.3. H&E staining

Animals were euthanized by CO_2 and eyes were immediately enucleated. Specimens were fixed in Excalibur's Z-Fix and processed (Sakura VIP) to paraffin. 4–5 micron sections were cut (AO820) and placed on slides. H&E staining was performed with Gill III hematoxylin

(StatLab Medical) and Alcoholic Eosin (StatLab Medical). Images were taken with a Nikon C2 confocal microscope system equipped with a Nikon Ds-Ri2 camera. Large scale images were generated using NIS elements AR 4.50 software with 5% overlap. ImageJ was used to count the nuclei of the outer nuclei layer at six different positions of the retina (Supplementary Fig 1). Nuclei of the outer nuclei layer were counted at each measurement point. The −3 and 3 positions were established by counting 20 nuclei in from the outermost edge. The −1 and 1 positions were defined 20 nuclei away from the optic nerve on the left and right side respectively. −2 and 2 positions were points in the middle of the other two measurements. Each measurement was replicated ten nuclei away from the first measurement. For each eye, ten sections were analyzed and the values averaged (20 measurements per position per eye) to obtain the final nuclei count (N=30 from three eyes from different animals for each group).

2.4. Isolation of retina, RPE/choroid, cornea, lens and optic nerve

All mice were euthanized through quick cervical dislocation. Eyes were enucleated and submerged in 3 ml cold HBSS on ice. Upon isolation, the eye was placed under the microscope on cold HBSS-soaked filter paper. The anterior half of the eye was removed to collect the cornea and lens. The posterior half was moved and submerged in a drop of 50 μl cold HBSS solution for retina isolation. Once the retina was removed, the remaining RPE/choroid was transferred to another drop of 50 μl cold HBSS. The lingering fat and muscle tissue was cleaned before harvesting the optic nerve and RPE/choroid. Once collected in microtubes, all tissues were snap-frozen in liquid N2. The procedure from enucleation to snap-frozen took about 15–20 seconds per lens, 18–25 seconds per cornea, 40–50 seconds per retina, 75–80 seconds per optic nerve and 80–90 seconds per RPE/choroid (N=4 from four different animals).

2.5. Mass spectrometry sample preparation

Frozen Samples were homogenized in cold 80% methanol (methanol:water (80:20 V/V), pre-cold on dry ice) using THb Handheld Tissue Homogenizer (Omni International, #THB115). After homogenization for 10–30 seconds, the samples were stored on dry ice for 30 min then centrifuged at 15000 RPM for 10 min at 4 °C. The supernatant was dried by the FreeZone 4.5 L freeze dryer (Labconco). The dried extract was either reconstituted for LC MS/MS or derivatized for GC MS. The pellets were dried and weighed for normalization.

2.6. Metabolite analysis by LC-MS/MS

Targeted metabolomics using LC-MS/MS was performed according to previous a validated procedure (Schelli et al., 2017; Xu et al., 2017; Zhong et al., 2017) with minor modifications. Briefly, a Thermo Fisher Scientific Dionex Ultimate 3000 HPLC system was used for chromatographic separation and analyte detection was performed using a TSQ-Quantiva triple quadrupole tandem mass spectrometer equipped with an electrospray ionization (ESI) source. Each sample was injected twice to perform detection in both negative and positive ionization modes. Regardless of ionization mode, chromatographic separations of targeted metabolites were performed on an Xbridge BEH hydrophilic interaction chromatography column (Waters Corporation, Milford, MA, 150×2.1 mm, 3.0 μm). HPLC separation was performed (0.30 mL/min) with the autosampler thermostatted to

4°C, and the column compartment to 40 °C. Mobile phase A consisted of 5 mM ammonium acetate prepared in 10% acetonitrile containing 0.2% acetic acid and mobile phase B was 5 mM ammonium acetate prepared in 90% acetonitrile containing 0.2% acetic acid. Total running time for both ionization modes was 20 min with chromatographic gradient separation (0–2 min, 70% B; 5 min, 30% B; 9 min, 30% B; 11 min, 70% B; 20 min, 70% B). The LC- MS/MS was controlled by Xcalliber version 2.0 (Thermo Fisher Scientific). Authentic standards corresponding to the measured metabolites were purchased from Sigma-Aldrich (Saint Louis, MO) or IROA Technologies (Boston, MA). Stable isotope-labeled amino acids (U-13C, 97–99%; U-15N, 97–99%) were purchased from Cambridge Isotope Laboratories (Tewksbury, MA). LC-MS grade acetonitrile, ammonium acetate, and acetic acid were all purchased from Fisher Scientific (Pittsburgh, PA). The targeted metabolic profiling was performed in selected-reaction-monitoring (SRM) mode, established by running multiple authentic chemical standards and then the combination of retention time and SRM transition from standards were used to detect and identify metabolites from biological samples. The 241 metabolites were selected according to our published work (Schelli et al., 2017; Zhu et al., 2015; Zhu et al., 2014). The detection parameters for these metabolites are listed in supplementary Table 1.

2.7. Metabolite analysis by GC MS

The extracts were derivatized by methoxyamine (Sigma-Aldrich, # 226904) at 37 °C for 90 min then derivatized by N,O-Bis(trimethylsilyl)trifluoroacetamide with trimethylchlorosilane (Sigma-Aldrich #15238) at 70 °C for 60 min. An Agilent 7890B/ 5977B GC/MS system with an Agilent DB-5MS column (30 m x 0.25 mm x 0.25 μm film) was used for GC separation and analysis of metabolites. Ultra-high- purity helium was the carrier gas at a constant flow rate of 1 mL/min. One microliter of sample was injected in split-less mode by the auto sampler. The temperature gradient started at 80 °C with a hold time of 2 min and increased at a rate of 10 °C/min to 180 °C, then at a rate of 5 °C/min to 240 °C, finally at a rate 25 °C/min to 290 °C where it was held for 9 min. The total run time was 35 min. The temperatures were set as follows: inlet 250 °C, transfer line 280 °C, ion source 230 °C, and quadrupole 150 °C. Mass spectra were collected from 50–500 m/z under selective ion monitoring mode (SRM). All of the metabolites were tested by using authentic standards and the parameters for target ions and retention time used for SRM was listed in supplementary Table 2. Myristic acid-d27 was added into each sample as the internal standard. The data was analyzed by Agilent MassHunter Quantitative Analysis Software.

2.8. Statistical analysis

Principle component analysis and volcano plot ($P<0.05$ with non-parametric test and fold change >1.2) were analyzed using MetaboAnalyst (http://www.metaboanalyst.ca/). Changed metabolites from Volcano plot were further enriched for pathways using Enrichment Analysis from MetaboAnalyst for significantly altered metabolic pathways. For univariate analysis, the significance of differences was determined by unpaired two-tailed t tests or analysis of variance with Bonferroni post hoc test. Data were mean ± SE. A p value < 0.05 was considered to be significant.

3. Results

3.1. Visual function declines and photoreceptor neurons decrease in the old animals

We evaluated visual function by electroretinography (ERG) of both the young and old mice. The animals were dark-adapted overnight and ERG a-wave and b-wave responses were measured over a range of flash intensities. The ERG responses increased with flash intensity (Fig 1). Old mice had significantly small dark-adapted (scotopic) a-wave and b-wave responses starting at −10 decibel (dB). For cone responses, old mice had smaller light-adapted (photopic) b-wave at all flash intensities (Fig 1C). To determine whether the decline of ERG response was due to loss of photoreceptors, we stained retinal sections with H &E and quantified the number of nuclei in the outer nuclear layer (ONL) at six different positions (Supplementary Fig 1 and Fig 1D-E). The number of nuclei in the ONL was sparse and significantly lower in the aging retina (Fig 1D-E), indicating loss of photoreceptors in the old mice.

3.2. Metabolic changes in the aged retina

To study the metabolic profile of the aging eye, we combined LC MS/MS and GC MS to target 297 metabolites from several major metabolic pathways (Supplementary Table 1-2). The selection of 297 metabolites is based on previous literature on targeted metabolomics (Zhu et al., 2014), our previous work on retinal metabolomics (Chao et al., 2017; Du et al., 2016) and the availability of standards. The quantified metabolite data from young and old retinas were evaluated by PCA analysis. Score plots separated the young and old into two different groups, indicating that the metabolic profile is different between these retinas. Volcano plots showed 68 significantly changed metabolites between young and old retinas (Supplementary Fig 2, Table 3). We enriched the metabolic pathways for these changed metabolites using MetaboAnalyst (http://www.metaboanalyst.ca/). Glucose metabolism (TCA cycle, gluconeogenesis, glycolysis, pentose phosphate pathway) and amino acid metabolism (malate-aspartate shuttle, aspartate and glutamate) were the major pathways that were affected (Fig 2B). For specific metabolites, we identified metabolites that were most decreased or increased in the aged retina (Fig 2 CD). Consistently, oxaloacetate, a critical metabolite in the TCA cycle and Malate-Aspartate Shuttle, was the most reduced. Metabolites in glycolysis and mitochondrial metabolism (Fructose 1,6-biphosphate (F- 1,6-BP), 2 phosphoglyceric acid (2-PG), 2-hydroxyglutarate (2-HG)) were diminished about half in old retinas, indicating that glucose utilization might be impaired. Carbohydrates including deoxyribose and glycerate, increased substantially in the old retinas. Remarkably, among the top fifteen increased metabolites in the old retina, seven were amino acids. Most of these amino acids are acetylated or methylated such as acetylcysteine and methylglutamate, suggesting that posttranslational modification is dysregulated in the aged retina.

3.3. Metabolic changes in the aged RPE/choroid

Since RPE is tightly bound to the choroid, we analyzed metabolites from the RPE/choroid complex. Multivariate analysis showed two distinctive groups for the metabolites from the young and old RPE/choroid in the score plots (Fig 3A). We identified 45 significantly changed metabolites by Volcano plot analysis (Supplementary Fig 3, Supplementary Table

4). Among these 45 metabolites, pathways in mitochondrial metabolism, glucose metabolism and amino acid metabolism were highly enriched (Fig 3B). Both NAD and riboflavin (a precursor for FAD) were depleted to less than half of the young levels in the aged RPE/choroid (Fig 3C). However, nicotinamide, the substrate for NAD synthesis, and the substrates for mitochondrial metabolism such as pyruvate and DHAP accumulated to higher levels in the old mice (Fig 3D), suggesting impaired mitochondrial energy metabolism. Additionally, leucine, 5- oxoproline (a metabolite in the glutathione cycle) and homocysteine were about 5 times lower in the old RPE/choroid, demonstrating that the utilization of these amino acids is severely impaired in the aged RPE/choroid (Fig 3C).

3.4. Metabolic changes in the aged lens

Lens metabolites in young and old mice could be divided into two distinctive groups in the score plots (Fig 4A). Volcano plots showed 54 metabolites were significantly different between these two groups (Supplementary Fig 4, Supplementary Table 5). Among the top enriched pathways, 60% were involved in amino acid metabolism such as taurine, alanine, methionine and tryptophan (Fig 4B). Taurine and hypotaurine are known to be abundant in the lens (Yanshole et al., 2014). Both hypotaurine and cystathionine, intermediates in taurine metabolism, decreased more than 70% in the aging lens (Fig 4C). Other amino acids and their intermediates such as deoxycarnitine (an intermediate in lysine and methionine metabolism), acetylalanine, kyneurenine (an intermediate for NAD synthesis from tryptophan), and methoxytryamine (an intermediate in phenylalanine and tyrosine metabolism) also were substantially decreased (Fig 4C). Additionally, the intermediates in glucose metabolism including glycolysis (F-1,6 BP) and mitochondrial TCA cycle (α-KG, malate and oxaloacetate) were diminished in the aging lens. Among the top increased metabolites, most are amino acids such as anthranilate (an intermediate for tryptophan), Cys-Gly and arginine, indicating that amino acid metabolism is severely disturbed in the aged lens.

3.5. Metabolic changes in the aged cornea

PCA analysis revealed significant metabolic differences between corneas from young and old mice. (Fig 5A). Among the 297 detected metabolites, we identified 45 changed metabolites in the aged cornea (Supplementary Fig 5, Supplementary Table 6). Taurine metabolism was the most enriched pathway (Fig 5B). Both taurine and cysteic acid decreased dramatically in the aged cornea while hypotaurine increased (Fig 5C-D). Additionally, the metabolism of other amino acids such as tryptophan and histidine also were highly enriched (Fig 5C-D). Different from lens, cholesterol was significantly lower and many methylated metabolites were upregulated, indicating there are some unique alterations in these pathways in the aged cornea.

3.6. Metabolic changes in the aged optic nerve

Similar to other aged ocular tissues, the aged optic nerve had a significantly different metabolic profile from the young optic nerve (Fig 6A). A total of 114 metabolites were changed in the volcano plot (Supplementary Fig 6, Supplementary Table 7). Besides glucose and amino acid metabolism, many of the changed metabolites were involved in lipid metabolism (Fig 6B-D). Among the top 15 downregulated metabolites, 11 were lipids

including cholesterol, fatty acid, phospholipid and steroids (Fig 6B). Acetylserotonin, a known neuroprotectant, decreased dramatically in the aged optic nerve (Fig 6B). Remarkably, erythritol, a sugar alcohol, increased 75 fold over the young optic nerve (Fig 6D). Glucose and its intermediates also increased significantly in the aged optic nerve. Similar to changes that occur in the aged cornea, many methylated metabolites such as methylated nucleotides and amino acids accumulated in the aged optic nerve (Fig 6D).

3.7. Common metabolites in aged ocular tissue

Among the changed metabolites in five aged ocular tissues we analyzed, no metabolite was changed in all tissues, indicating the specificity for each tissue. However, there were 31 metabolites that were changed in at least three tissues (Supplementary Table 8). Six of them were changed in four tissues (Fig 7A). It is noteworthy that 1-methylnicotinamide (1-methylNAA) was the only metabolite that accumulated to higher levels in all four tissues. 1-methylNAA is produced by methylation of nicotinamide, a precursor for NAD biosynthesis. This is important because NAD is a key cofactor that links cellular redox states with energy metabolism. NAD accumulated to higher levels with aging in all tissues except RPE, where it was depleted with aging (Fig 7A-B). Strikingly, other methylated metabolites such as 3-methylhistidine, trimethyllysine and 5'-methylthioadenosine accumulated to higher levels in the aging tissues, indicating dysregulated methyl group metabolism. Carnitine plays an important role in transporting long-chain CoA (derived from long-chain fatty acid) into the mitochondria for oxidation. Interestingly, the level of both carnitine and the long chain fatty acid, oleate, changed with aging in four aged tissues (Fig 7A), indicating dysregulation of lipid metabolism.

4. Discussion

In this report, we have described how the metabolome is altered in the aging eye in mice. Our ERG analysis confirms that visual function and the number of photoreceptors decline in the aging eye. Among the 297 metabolites we detected, 45–114 change significantly in aging eye tissues. The changes are the largest in the neuronal tissues (retina and optic nerve) and smaller in other tissues. Mitochondrial metabolism (TCA cycle, electron transport chain and electron shuttle) and glucose metabolism (glycolysis and gluconeogenesis) are the pathways most affected by aging in retina, RPE/choroid, optic nerve and lens. NAD and its derivative 1-methylNAA are changed in four aging ocular tissues. Besides 1- methylNAA, the accumulation of other methylated metabolites also is common in the aging retina, cornea, optic nerve and lens. In the aging cornea and lens, metabolites in taurine metabolism are strikingly influenced. Each of these substantial alterations in the metabolome may contribute to or may be caused by age-associated neuronal cell loss and declining visual function.

4.1. Mitochondrial metabolism in the aging eye

Metabolites in mitochondrial metabolism occur in many of the tissues in the aging eye. These changed metabolites include intermediates in TCA cycle (oxaloacetate, a-ketoglutarate, citrate and malate), electron transport chain (NAD and its derivatives or precursors (nicotinamide, 1-methylNAA, trigoneline and tryptophan); FAD and its precursor

riboflavin) and malate-aspartate shuttle (Fig 2-7, supplementary Table 3-8). Mitochondria are abundant in the retina, RPE and optic nerve. To be transparent for light refraction, both the cornea and lens have fewer mitochondria, which are limited to endothelial cells and epithelial cells. Consistently, we found the mitochondrial metabolic changes occur mostly in the aging retina, RPE and optic nerve. Mitochondrial dysfunction has been identified as an important target for aging and age-related eye diseases (Barot et al., 2011; Lefevere et al., 2017; Lopez Sanchez et al., 2016). The disruption of mitochondrial intermediate metabolism and electron transport could reduce energy production and increase the generation of reactive oxygen species, resulting in oxidative stress and damage to the aging eyes. Additionally, several mitochondrial TCA cycle intermediates also decrease in the aging lens, indicating that lens epithelial cells are dysfunctional in mitochondrial energy metabolism. These results are consistent with a recent report that mitochondrial oxygen metabolism is diminished in the older human lens epithelial cells (Kubota et al., 2016). Mitochondria-derived oxidative stress has been regarded as an important target for cataract treatment (Babizhayev and Yegorov, 2016).

1-methylNAA accumulates to higher levels in all of the aging tissues except RPE. 1-methylNAA is produced from nicotinamide N-methyltransferase (NNMT) by transferring a methyl group from S-adenosylmethionine (SAM) onto nicotinamide (Fig 7B). Since SAM is a universal methyl donor and nicotinamide is an important precursor for NAD^+ (Pissios, 2017), the enhanced production of 1-methylNAA can affect the activity of NAD^+-dependent enzymes and SAM-dependent methyltransferases. A recent study showed that both NNMT activity and the level of 1-methylNAA are sensitive to energy deficit and their upregulation can shift human muscle from glucose metabolism to lipid metabolism (Strom et al., 2018). NNMT expression increases in white adipose tissue and liver of obese and diabetic mice. Knockdown of NNMT augments cellular energy expenditure, upregulates histone methylation and protects against diet-induced obesity (Kraus et al., 2014). In the urine metabolome from aging mice, 1-methylNAA is the top increased metabolite (Calvani et al., 2014). Our results suggest that 1-methylNAA might be a hallmark for the aging eye. It may be associated with mitochondrial deficiency and stimulation of lipid metabolism that occur with aging.

4.2.   Glucose and lipid metabolism of the aging eye

Glycolysis is a predominant metabolic pathway in both the retina and lens (Ait-Ali et al., 2015; Gillis et al., 1981; Hejtmancik et al., 2015; Hurley et al., 2015; Kanow et al., 2017). The decrease of glycolytic intermediates in the aging retina and lens indicates a deficiency in glucose metabolism. In contrast, in the RPE and optic nerve, glucose and glycolytic intermediates accumulate to higher levels while lipids including fatty acids, cholesterol, phospholipids and steroids become depleted in the aging RPE and optic nerve. Since mitochondrial oxidative phosphorylation is very active in the RPE and optic nerve, our findings suggest that the mitochondria of the aging RPE and optic nerve do not utilize glucose efficiently to accumulate glycolytic intermediates. Aging mitochondria may shift to lipid metabolism as fatty acids are depleted in the aging RPE and optic nerve. Additionally, age-related formation of lipofuscin and perturbed cholesterol efflux (Crouch et al., 2015;

Dolman et al., 1980; Fernandez de Castro et al., 2013; Lakkaraju et al., 2007) also may contribute to the depletion of lipids.

4.3. Methylated metabolites in the aging eye

In addition to 1-methylNAA, many other methylated metabolites such as 3-methylglutarate, 3- methylhistidine, trimethyllysine and 5'-methylthioadenosine accumulate in the aging retina, cornea, optic nerve and lens. 3-methylglutarate, an intermediate in leucine degradation, can disrupt mitochondrial function, induce oxidative stress and damage DNA in the rat brain (Colin-Gonzalez et al., 2016; da Rosa et al., 2015). The formation of 1-methylNAA, 3-methylhistidine, trimethyllysine and 5'- methylthioadenosine relies on methyltransferases which transfer methyl groups from SAM. Epigenetic regulation by methylation of DNA and histone also requires activated methyl groups. Lower levels of global DNA methylation have been reported in various aging tissues in animals and humans (Liu et al., 2003; Unnikrishnan et al., 2018). We speculate that the consumption of methyl groups to generate these methylated metabolites may limit the availability of SAM for DNA methylation in the aging eye. In aged skeletal muscle, 3-methylhistidine, a marker for muscle protein breakdown increases substantially (Sato et al., 2017). Elevated levels of 5'-methylthioadenosine (MTA) appears in urine of older people with diabetes. Interestingly, large amounts of trimethyllysine accumulate in intracellular deposits from patients with Juvenile ceroid lipofuscinosis, a hereditary disorder characterized by progressive visual loss, seizures, cognitive and psychomotor deterioration (Katz and Rodrigues, 1991). These reports and our findings suggest that the increase of these methylated metabolites might disrupt the balance of methyl group metabolism to impact epigenetic regulation, resulting in aging-associated structural changes. Further studies are needed to elucidate the roles of these methylated metabolites in the eye.

4.4. Taurine metabolism in the aging cornea and lens

Taurine metabolism is the most altered pathway in both the aged cornea and aged lens. Taurine is one of the most abundant amino acids in the retina, cornea and lens (Ripps and Shen, 2012). Different from all the other amino acids, taurine has a sulfonic acid group instead of the classic carboxylic group. It is an important cytoprotective metabolite involved in anti-oxidative stress, anti-inflammation, osmoprotection, regeneration and regulation of Ca^{2+} concentration (Ripps and Shen, 2012; Rusciano et al., 2016). In the rat, the amount of taurine level declines with age in the cornea and lens (Baskin et al., 1977; Yanshole et al., 2014). Topical taurine application can contribute to epithelial wound healing and taurine is typically included in contact lens cleaning solutions to protect the corneal stroma and epithelium (Funke et al., 2012; Rusciano et al., 2016). The major route for the biosynthesis of taurine is from methionine and cysteine, and requires the oxidation of hypotaurine or cysteic acid to taurine. Cysteine sulfoinic acid decarboxylase (CSAD) is a key enzyme in taurine biosynthesis from hypotaurine and it has the highest activity in the cornea among ocular tissues (Heinamaki, 1988). In the aging cornea, the amount of taurine and cysteic acid decreases substantially while hypotaurine increases, suggesting the aging cornea might have impaired CSAD activity and compensate with CSAD-independent taurine synthesis from cysteic acid. However, in the aging lens, hypotaurine and cystathionine (a precursor for

cysteine) are depleted while cysteic acid accumulates, suggesting different mechanisms for dysregulated taurine metabolism between the cornea and lens.

4.5. Future directions

Among different aging ocular tissues, alterations of methylated metabolites and mitochondrial metabolites are the most striking and common features in the metabolic profile of aging. It will be interesting to investigate whether these two common changes are inter-connected, whether these alterations are the cause or the effect of aging in the eye, how these metabolites are changed in age-associated ocular diseases and whether manipulation of genes responsible for the methylations will slow down or prevent visual decline in animal models *in vivo*. Furthermore, the targeted metabolomics in this study provides only a snapshot of metabolism by measuring steady state metabolites without dynamic information, *e.g.* the accumulation of metabolites can be caused by either more synthesis or less degradation. Future studies using tracers to label the reactions in mitochondrial metabolism and/or methylation are critical to understand the mechanisms for these metabolic alterations. Additionally, metabolites can be exported out of cells and transported between ocular tissues (Chao et al., 2017; Kanow et al., 2017). How the changes in the tissue metabolomes that we report here impact metabolites in the vitreous also will be important to investigate, as it could potentially be translated into diagnosis or prognosis in patients.

5. Conclusions

In conclusion, aging has a remarkable metabolic signature in the various tissues of the eye, including dysregulated mitochondrial metabolism, shifted patterns in the utilization of glucose and lipid, accumulated methylated metabolites and impaired taurine metabolism. These findings should help to reveal the biochemical mechanisms in age-related ocular changes and the decline of visual function, identify novel markers for the aging eye and shed light on anti-aging research.

Supplementary Material

Refer to Web version on PubMed Central for supplementary material.

Acknowledgement:

References

Ait-Ali N, Fridlich R, Millet-Puel G, Clerin E, Delalande F, Jaillard C, Blond F, Perrocheau L, Reichman S, Byrne LC, Olivier-Bandini A, Bellalou J, Moyse E, Bouillaud F, Nicol X, Dalkara D, van Dorsselaer A, Sahel JA, Leveillard T, 2015 Rod-derived cone viability factor promotes cone survival by stimulating aerobic glycolysis. Cell 161(4), 817–832. [PubMed: 25957687]

Babizhayev MA, Yegorov YE, 2016 Reactive Oxygen Species and the Aging Eye: Specific Role of Metabolically Active Mitochondria in Maintaining Lens Function and in the Initiation of the Oxidation- Induced Maturity Onset Cataract--A Novel Platform of Mitochondria-Targeted Antioxidants With Broad Therapeutic Potential for Redox Regulation and Detoxification of Oxidants in Eye Diseases. American journal of therapeutics 23(1), e98–117. [PubMed: 21048433]

Barot M, Gokulgandhi MR, Mitra AK, 2011 Mitochondrial dysfunction in retinal diseases. Current eye research 36(12), 1069–1077. [PubMed: 21978133]

Baskin SI, Cohn EM, Kocsis, 1977 The effect of age on taurine levels in eye tissues. Experimental eye research 24(3), 315–319. [PubMed: 852529]

Cajka T, Fiehn O, 2016 Toward Merging Untargeted and Targeted Methods in Mass Spectrometry-Based Metabolomics and Lipidomics. Analytical chemistry 88(1), 524–545. [PubMed: 26637011]

Calvani R, Brasili E, Pratico G, Capuani G, Tomassini A, Marini F, Sciubba F, Finamore A, Roselli M, Marzetti E, Miccheli A, 2014 Fecal and urinary NMR-based metabolomics unveil an aging signature in mice. Experimental gerontology 49, 5–11. [PubMed: 24184118]

Cavallotti C, Cavallotti D, Pescosolido N, Pacella E, 2003 Age-related changes in rat optic nerve: morphological studies. Anatomia, histologia, embryologia 32(1), 12–16.

Chader GJ, Taylor A, 2013 Preface: The aging eye: normal changes, age-related diseases, and sightsaving approaches. Investigative ophthalmology & visual science 54(14), ORSF1–4. [PubMed: 24335060]

Chao JR, Knight K, Engel AL, Jankowski C, Wang Y, Manson MA, Gu H, Djukovic D, Raftery D, Hurley JB, Du J, 2017 Human retinal pigment epithelial cells prefer proline as a nutrient and transport metabolic intermediates to the retinal side. The Journal of biological chemistry 292(31), 12895–12905. [PubMed: 28615447]

Colin-Gonzalez AL, Paz-Loyola AL, de Lima ME, Galvan-Arzate S, Seminotti B, Ribeiro CA, Leipnitz G, Souza DO, Wajner M, Santamaria A, 2016 Experimental Evidence that 3-Methylglutaric Acid Disturbs Mitochondrial Function and Induced Oxidative Stress in Rat Brain Synaptosomes: New Converging Mechanisms. Neurochemical research 41(10), 2619–2626. [PubMed: 27278758]

Crouch RK, Koutalos Y, Kono M, Schey K, Ablonczy Z, 2015 A2E and Lipofuscin. Progress in molecular biology and translational science 134, 449–463. [PubMed: 26310170]

da Rosa MS, Scaini G, Damiani AP, Longaretti LM, Pereira M, Seminotti B, Zapelini HG, Schuck PF, Streck EL, de Andrade VM, Wajner M, Leipnitz G, 2015 Evidence that 3-hydroxy-3-methylglutaric and 3-methylglutaric acids induce DNA damage in rat striatum. Metabolic brain disease 30(4), 1055–1062. [PubMed: 25939283]

Delcourt C, Korobelnik JF, Barberger-Gateau P, Delyfer MN, Rougier MB, Le Goff M, Malet F, Colin J, Dartigues JF, 2010 Nutrition and age-related eye diseases: the Alienor (Antioxydants, Lipides Essentiels, Nutrition et maladies OculaiRes) Study. The journal of nutrition, health & aging 14(10), 854–861.

Delori FC, Goger DG, Dorey CK, 2001 Age-related accumulation and spatial distribution of lipofuscin in RPE of normal subjects. Investigative ophthalmology & visual science 42(8), 1855–1866. [PubMed: 11431454]

Dhillon RS, Denu JM, 2017 Using comparative biology to understand how aging affects mitochondrial metabolism. Molecular and cellular endocrinology 455, 54–61. [PubMed: 28025033]

Dolman CL, McCormick AQ, Drance SM, 1980 Aging of the optic nerve. Arch Ophthalmol 98(11), 2053–2058. [PubMed: 7436843]

Du J, Rountree A, Cleghorn WM, Contreras L, Lindsay KJ, Sadilek M, Gu H, Djukovic D, Raftery D, Satrustegui J, Kanow M, Chan L, Tsang SH, Sweet IR, Hurley JB, 2016 Phototransduction Influences Metabolic Flux and Nucleotide Metabolism in Mouse Retina. The Journal of biological chemistry 291(9), 4698–4710. [PubMed: 26677218]

Duncan G, Wormstone IM, Davies PD, 1997 The aging human lens: structure, growth, and physiological behaviour. The British journal of ophthalmology 81(10), 818–823. [PubMed: 9486018]

Elizabeth Rakoczy P, Yu MJ, Nusinowitz S, Chang B, Heckenlively JR, 2006 Mouse models of age-related macular degeneration. Experimental eye research 82(5), 741–752. [PubMed: 16325179]

Feng Z, Hanson RW, Berger NA, Trubitsyn A, 2016 Reprogramming of energy metabolism as a driver of aging. Oncotarget 7(13), 15410–15420. [PubMed: 26919253]

Fernandez de Castro JP, Mullins RF, Manea AM, Hernandez J, Wallen T, Kuehn MH, 2013 Lipofuscin in human glaucomatous optic nerves. Experimental eye research 111, 61–66. [PubMed: 23567206]

Ferrington DA, Ebeling MC, Kapphahn RJ, Terluk MR, Fisher CR, Polanco JR, Roehrich H, Leary MM, Geng Z, Dutton JR, Montezuma SR, 2017 Altered bioenergetics and enhanced resistance to oxidative stress in human retinal pigment epithelial cells from donors with age-related macular degeneration. Redox biology 13, 255–265. [PubMed: 28600982]

Funke S, Azimi D, Wolters D, Grus FH, Pfeiffer N, 2012 Longitudinal analysis of taurine induced effects on the tear proteome of contact lens wearers and dry eye patients using a RP-RP-Capillary-HPLC- MALDI TOF/TOF MS approach. Journal of proteomics 75(11), 3177–3190. [PubMed: 22480906]

Gambato C, Longhin E, Catania AG, Lazzarini D, Parrozzani R, Midena E, 2015 Aging and corneal layers: an in vivo corneal confocal microscopy study. Graefe's archive for clinical and experimental ophthalmology = Albrecht von Graefes Archiv fur klinische und experimentelle Ophthalmologie 253(2), 267–275.

Gillis MK, Chylack LT, Jr., Cheng HM, 1981 Age and the control of glycolysis in the rat lens. Investigative ophthalmology & visual science 20(4), 457–466. [PubMed: 6452426]

Gipson IK, 2013 Age-related changes and diseases of the ocular surface and cornea. Investigative ophthalmology & visual science 54(14), ORSF48–53. [PubMed: 24335068]

He Y, Ge J, Burke JM, Myers RL, Dong ZZ, Tombran-Tink J, 2010 Mitochondria impairment correlates with increased sensitivity of aging RPE cells to oxidative stress. Journal of ocular biology, diseases, and informatics 3(3), 92–108.

He Y, Tombran-Tink J, 2010 Mitochondrial decay and impairment of antioxidant defenses in aging RPE cells. Advances in experimental medicine and biology 664, 165–183. [PubMed: 20238015]

Heinamaki AA, 1988 Endogenous synthesis of taurine and GABA in rat ocular tissues. Acta chemica Scandinavica. Series B: Organic chemistry and biochemistry 42(1), 39–42.

Hejtmancik JF, Riazuddin SA, McGreal R, Liu W, Cvekl A, Shiels A, 2015 Lens Biology and Biochemistry. Progress in molecular biology and translational science 134, 169–201. [PubMed: 26310155]

Hurley JB, Lindsay KJ, Du J, 2015 Glucose, lactate, and shuttling of metabolites in vertebrate retinas. Journal of neuroscience research 93(7), 1079–1092. [PubMed: 25801286]

Johnson M, Dabholkar A, Huang JD, Presley JB, Chimento MF, Curcio CA, 2007 Comparison of morphology of human macular and peripheral Bruch's membrane in older eyes. Current eye research 32(9), 791–799. [PubMed: 17882712]

Kanow MA, Giarmarco MM, Jankowski CS, Tsantilas K, Engel AL, Du J, Linton JD, Farnsworth CC, Sloat SR, Rountree A, Sweet IR, Lindsay KJ, Parker ED, Brockerhoff SE, Sadilek M, Chao JR, Hurley JB, 2017 Biochemical adaptations of the retina and retinal pigment epithelium support a metabolic ecosystem in the vertebrate eye. eLife 6.

Katz ML, Rodrigues M, 1991 Juvenile ceroid lipofuscinosis. Evidence for methylated lysine in neural storage body protein. The American journal of pathology 138(2), 323–332. [PubMed: 1899540]

Kraus D, Yang Q, Kong D, Banks AS, Zhang L, Rodgers JT, Pirinen E, Pulinilkunnil TC, Gong F, Wang YC, Cen Y, Sauve AA, Asara JM, Peroni OD, Monia BP, Bhanot S, Alhonen L, Puigserver P, Kahn BB, 2014 Nicotinamide N-methyltransferase knockdown protects against diet- induced obesity. Nature 508(7495), 258–262. [PubMed: 24717514]

Kubota M, Shui YB, Liu M, Bai F, Huang AJ, Ma N, Beebe DC, Siegfried CJ, 2016 Mitochondrial oxygen metabolism in primary human lens epithelial cells: Association with age, diabetes and glaucoma. Free radical biology & medicine 97, 513–519. [PubMed: 27445101]

Lakkaraju A, Finnemann SC, Rodriguez-Boulan E, 2007 The lipofuscin fluorophore A2E perturbs cholesterol metabolism in retinal pigment epithelial cells. Proceedings of the National Academy of Sciences of the United States of America 104(26), 11026–11031. [PubMed: 17578916]

Lee WH, Higuchi H, Ikeda S, Macke EL, Takimoto T, Pattnaik BR, Liu C, Chu LF, Siepka SM, Krentz KJ, Rubinstein CD, Kalejta RF, Thomson JA, Mullins RF, Takahashi JS, Pinto LH, Ikeda A, 2016 Mouse Tmem135 mutation reveals a mechanism involving mitochondrial dynamics that leads to age-dependent retinal pathologies. eLife 5.

Lefevere E, Toft-Kehler AK, Vohra R, Kolko M, Moons L, Van Hove I, 2017 Mitochondrial dysfunction underlying outer retinal diseases. Mitochondrion 36, 66–76. [PubMed: 28365408]

Lei Y, Garrahan N, Hermann B, Fautsch MP, Johnson DH, Hernandez MR, Boulton M, Morgan JE, 2011 Transretinal degeneration in ageing human retina: a multiphoton microscopy analysis. The British journal of ophthalmology 95(5), 727–730. [PubMed: 21183516]

Li CM, Chung BH, Presley JB, Malek G, Zhang X, Dashti N, Li L, Chen J, Bradley K, Kruth HS, Curcio CA, 2005 Lipoprotein-like particles and cholesteryl esters in human Bruch's membrane: initial characterization. Investigative ophthalmology & visual science 46(7), 2576–2586. [PubMed: 15980251]

Lin JB, Tsubota K, Apte RS, 2016 A glimpse at the aging eye. NPJ aging and mechanisms of disease 2, 16003. [PubMed: 28721262]

Liu L, Wylie RC, Andrews LG, Tollefsbol TO, 2003 Aging, cancer and nutrition: the DNA methylation connection. Mechanisms of ageing and development 124(10–12), 989–998. [PubMed: 14659588]

Lopez Sanchez MI, Crowston JG, Mackey DA, Trounce IA, 2016 Emerging Mitochondrial Therapeutic Targets in Optic Neuropathies. Pharmacology & therapeutics 165, 132–152. [PubMed: 27288727]

Lott LA, Schneck ME, Haegerstrom-Portnoy G, Brabyn JA, 2010 Non-standard vision measures predict mortality in elders: the Smith-Kettlewell Institute (SKI) study. Ophthalmic epidemiology 17(4), 242–250. [PubMed: 20642347]

Maresca A, la Morgia C, Caporali L, Valentino ML, Carelli V, 2013 The optic nerve: a "mito-window" on mitochondrial neurodegeneration. Molecular and cellular neurosciences 55, 62–76. [PubMed: 22960139]

Mills KF, Yoshida S, Stein LR, Grozio A, Kubota S, Sasaki Y, Redpath P, Migaud ME, Apte RS, Uchida K, Yoshino J, Imai SI, 2016 Long-Term Administration of Nicotinamide Mononucleotide Mitigates Age-Associated Physiological Decline in Mice. Cell metabolism 24(6), 795–806. [PubMed: 28068222]

Mustonen RK, McDonald MB, Srivannaboon S, Tan AL, Doubrava MW, Kim CK, 1998 Normal human corneal cell populations evaluated by in vivo scanning slit confocal microscopy. Cornea 17(5), 485–492. [PubMed: 9756442]

Nadal-Nicolas FM, Vidal-Sanz M, Agudo-Barriuso M, 2018 The aging rat retina: from function to anatomy. Neurobiology of aging 61, 146–168. [PubMed: 29080498]

Pennesi ME, Neuringer M, Courtney RJ, 2012 Animal models of age related macular degeneration. Molecular aspects of medicine 33(4), 487–509. [PubMed: 22705444]

Pissios P, 2017 Nicotinamide N-Methyltransferase: More Than a Vitamin B3 Clearance Enzyme. Trends in endocrinology and metabolism: TEM 28(5), 340–353. [PubMed: 28291578]

Ripps H, Shen W, 2012 Review: taurine: a "very essential" amino acid. Molecular vision 18, 2673–2686. [PubMed: 23170060]

Rohrer B, Bandyopadhyay M, Beeson C, 2016 Reduced Metabolic Capacity in Aged Primary Retinal Pigment Epithelium (RPE) is Correlated with Increased Susceptibility to Oxidative Stress. Advances in experimental medicine and biology 854, 793–798. [PubMed: 26427491]

Rusciano D, Roszkowska AM, Gagliano C, Pezzino S, 2016 Free amino acids: an innovative treatment for ocular surface disease. European journal of pharmacology 787, 9–19. [PubMed: 27090927]

Salvi SM, Akhtar S, Currie Z, 2006 Ageing changes in the eye. Postgraduate medical journal 82(971), 581–587. [PubMed: 16954455]

Sarna T, Burke JM, Korytowski W, Rozanowska M, Skumatz CM, Zareba A, Zareba M, 2003 Loss of melanin from human RPE with aging: possible role of melanin photooxidation. Experimental eye research 76(1), 89–98. [PubMed: 12589778]

Sato T, Ito Y, Nagasawa T, 2017 L-Lysine suppresses myofibrillar protein degradation and autophagy in skeletal muscles of senescence-accelerated mouse prone 8. Biogerontology 18(1), 85–95. [PubMed: 27752791]

Schelli K, Rutowski J, Roubidoux J, Zhu J, 2017 Staphylococcus aureus methicillin resistance detected by HPLC-MS/MS targeted metabolic profiling. Journal of chromatography. B, Analytical technologies in the biomedical and life sciences 1047, 124–130. [PubMed: 27316783]

Stahon KE, Bastian C, Griffith S, Kidd GJ, Brunet S, Baltan S, 2016 Age-Related Changes in Axonal and Mitochondrial Ultrastructure and Function in White Matter. The Journal of neuroscience : the official journal of the Society for Neuroscience 36(39), 9990–10001. [PubMed: 27683897]

Strom K, Morales-Alamo D, Ottosson F, Edlund A, Hjort L, Jorgensen SW, Almgren P, Zhou Y, Martin-Rincon M, Ekman C, Perez-Lopez A, Ekstrom O, Perez-Suarez I, Mattiasson M, de Pablos- Velasco P, Oskolkov N, Ahlqvist E, Wierup N, Eliasson L, Vaag A, Groop L, Stenkula KG, Fernandez C, Calbet JAL, Holmberg HC, Hansson O, 2018 N(1)-methylnicotinamide is a signalling molecule produced in skeletal muscle coordinating energy metabolism. Scientific reports 8(1), 3016. [PubMed: 29445118]

Unnikrishnan A, Hadad N, Masser DR, Jackson J, Freeman WM, Richardson A, 2018 Revisiting the genomic hypomethylation hypothesis of aging. Annals of the New York Academy of Sciences.

Weinrich TW, Coyne A, Salt TE, Hogg C, Jeffery G, 2017 Improving mitochondrial function significantly reduces metabolic, visual, motor and cognitive decline in aged Drosophila melanogaster. Neurobiology of aging 60, 34–43. [PubMed: 28917665]

Whitcomb EA, Shang F, Taylor A, 2013 Common cell biologic and biochemical changes in aging and age-related diseases of the eye: toward new therapeutic approaches to age-related ocular diseases. Investigative ophthalmology & visual science 54(14), ORSF31–36. [PubMed: 24335065]

Williams PA, Harder JM, Foxworth NE, Cochran KE, Philip VM, Porciatti V, Smithies O, John SW, 2017 Vitamin B3 modulates mitochondrial vulnerability and prevents glaucoma in aged mice. Science 355(6326), 756–760. [PubMed: 28209901]

Xu M, Zhong F, Zhu J, 2017 Evaluating metabolic response to light exposure in Lactobacillus species via targeted metabolic profiling. Journal of microbiological methods 133, 14–19. [PubMed: 27974228]

Yanshole VV, Snytnikova OA, Kiryutin AS, Yanshole LV, Sagdeev RZ, Tsentalovich YP, 2014 Metabolomics of the rat lens: a combined LC-MS and NMR study. Experimental eye research 125, 71–78. [PubMed: 24910091]

Zeiss CJ, 2010 Animals as models of age-related macular degeneration: an imperfect measure of the truth. Veterinary pathology 47(3), 396–413. [PubMed: 20382825]

Zhong F, Xu M, Bruno RS, Ballard KD, Zhu J, 2017 Targeted High Performance Liquid Chromatography Tandem Mass Spectrometry-based Metabolomics differentiates metabolic syndrome from obesity. Exp Biol Med (Maywood) 242(7), 773–780. [PubMed: 28299975]

Zhu J, Djukovic D, Deng L, Gu H, Himmati F, Abu Zaid M, Chiorean EG, Raftery D, 2015 Targeted serum metabolite profiling and sequential metabolite ratio analysis for colorectal cancer progression monitoring. Analytical and bioanalytical chemistry 407(26), 7857–7863. [PubMed: 26342311]

Zhu J, Djukovic D, Deng L, Gu H, Himmati F, Chiorean EG, Raftery D, 2014 Colorectal cancer detection using targeted serum metabolic profiling. Journal of proteome research 13(9), 4120–4130. [PubMed: 25126899]
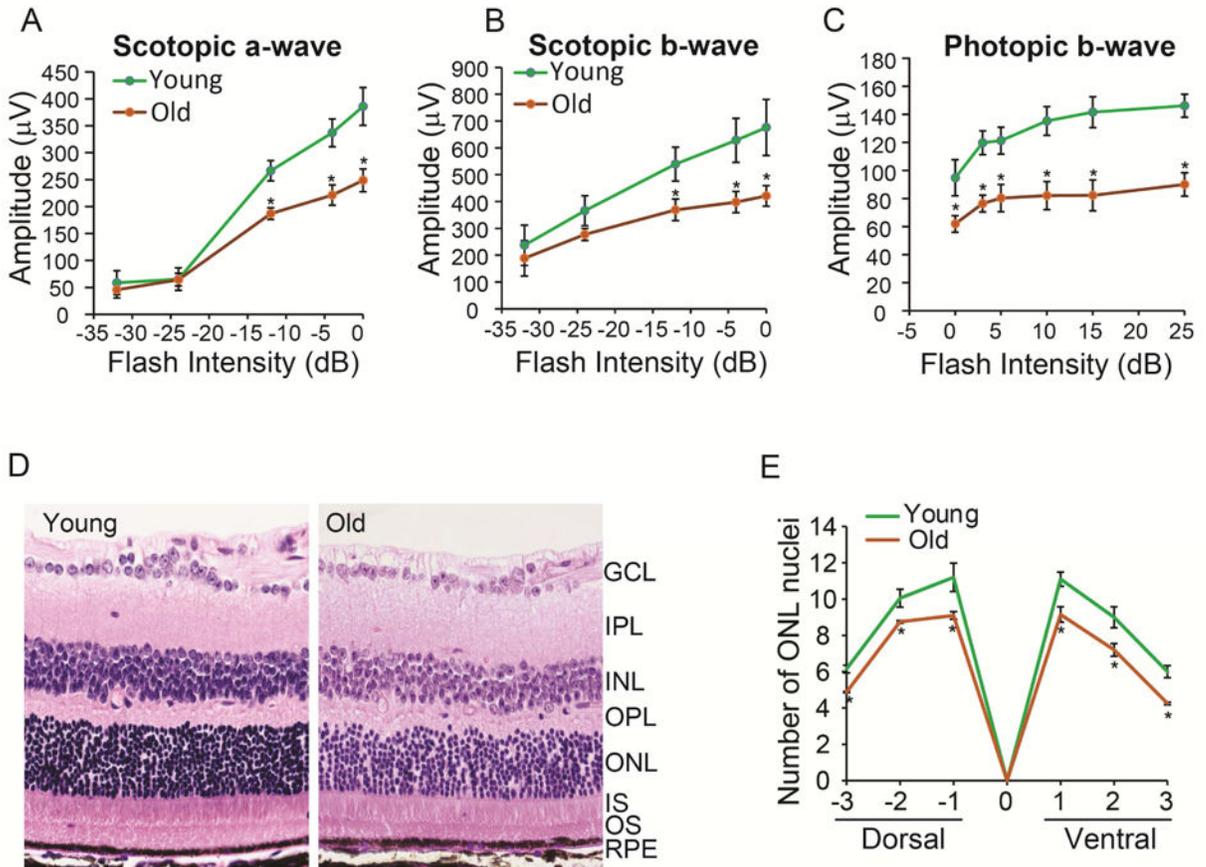
Highlights

45–114 metabolites are changed in the aging retina, RPE, lens, cornea and optic nerve
Altered mitochondrial metabolism and glucose metabolism in the aging ocular tissue
NAD and 1-methylnicotinamide are altered in four of aging ocular tissue Taurine
metabolism are the top influenced pathway in the aged lens and cornea

Figure 1. Aging causes a decline in ERG response and a reduction in the number of photoreceptors.

Dark-adapted mice were stimulated with different flash intensities. The average response of (A) scotopic a-wave, (B) scotopic b-wave and (C) photopic b-wave decreased in older mice. *$P<0.05$, N=10 from five animals for each group. (D) A representative H&E staining from young and old retinas at the −1 position. OS, outer segments; IS, inner segments; ONL, outer nuclear layer; OPL, outer plexiform layer; INL, inner nuclear layer; IPL, inner plexiform layer; GCL, ganglion layer. (D) The number of nuclei in the ONL in the retina. *$P<0.05$, N=30 from three animals for each group.
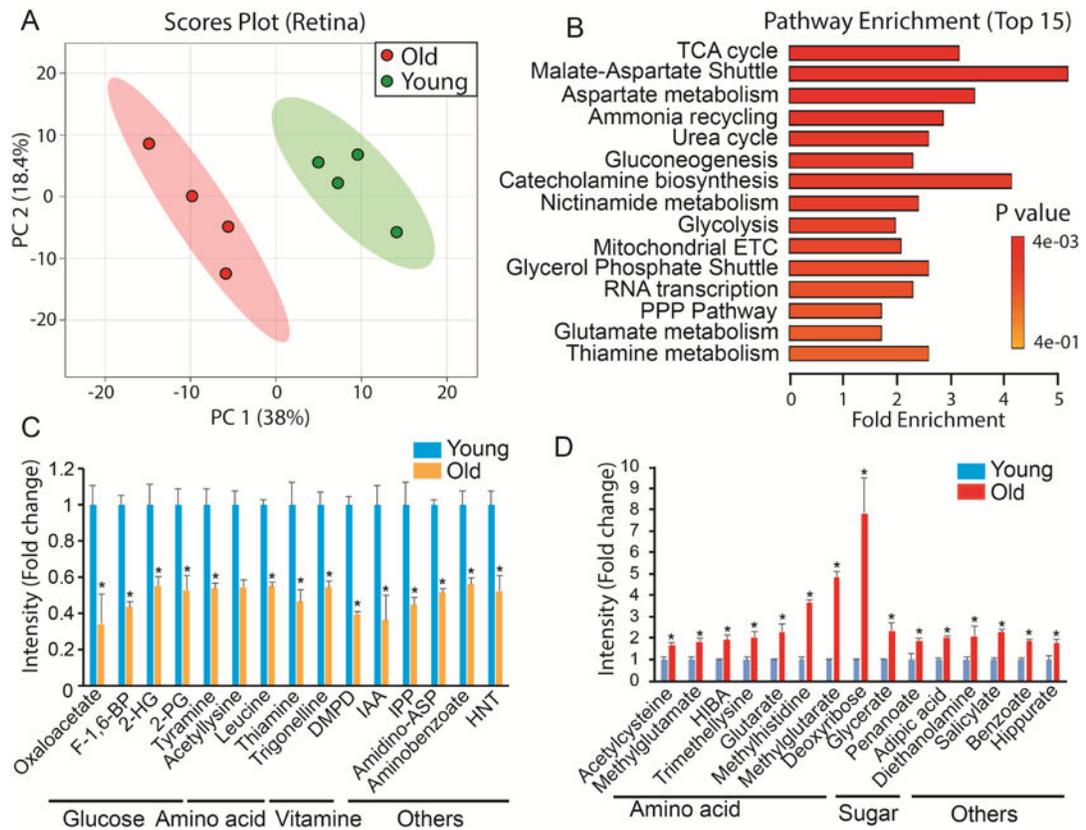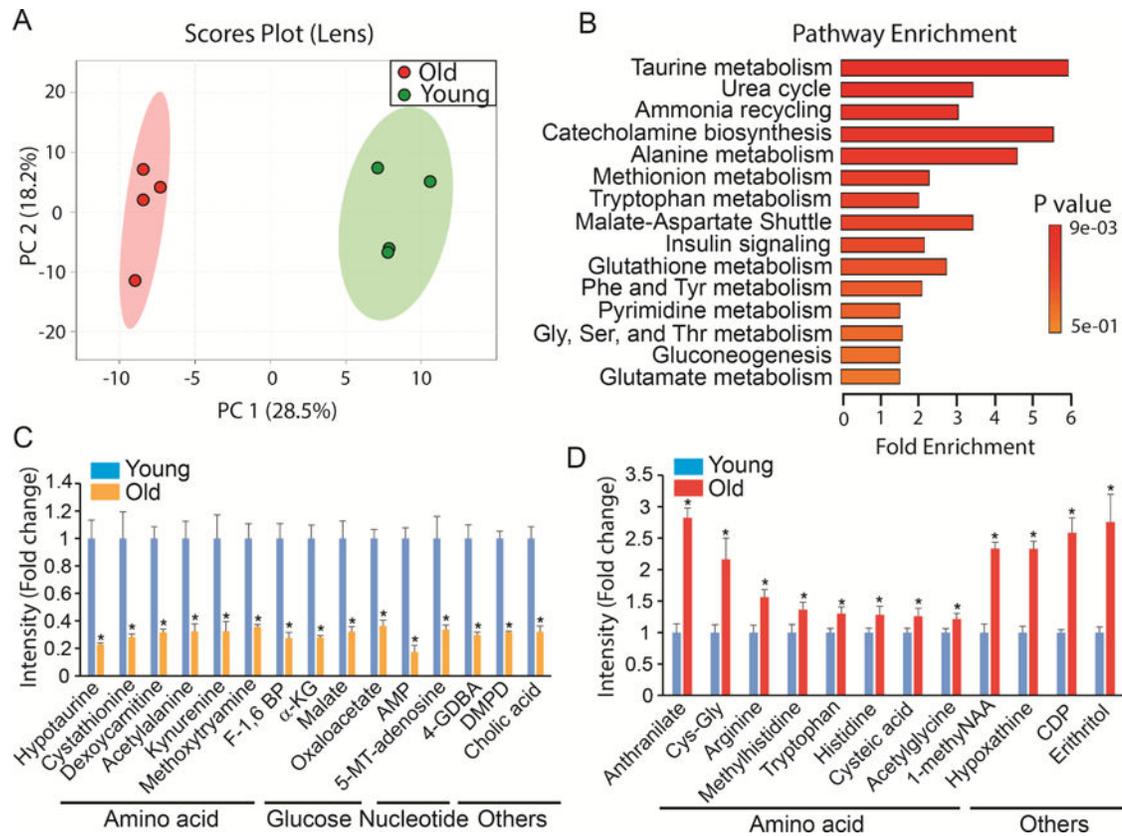
Figure 2. Differential metabolic profile between young and old retinas.
(A) Metabolites from young and old retinas were separated into two different groups in Scores Plot by PCA. (B) Top enriched pathways from significantly changed metabolites. ETC, electron transport chain; PPP, pentose phosphate. (C) Top decreased metabolites in old retinas. 2-HG, 2-hydroxyglutarate; 2-PG, 2-Phosphoglyceric Acid; DMPD, N,N-Dimethyl-1,4-Phenylenediamine; IAA, Indole-3-Acetic Acid; IPP, Isopentyl Pyrophosphate; Amidino-ASP, N-Amidino-L-Aspartate; HNT, 1-Hydroxy-2-Naphthoate. (D) Top increased metabolites in old retinas. Data report fold change of ion intensity of the old vs the young. N=4 from four different animals.
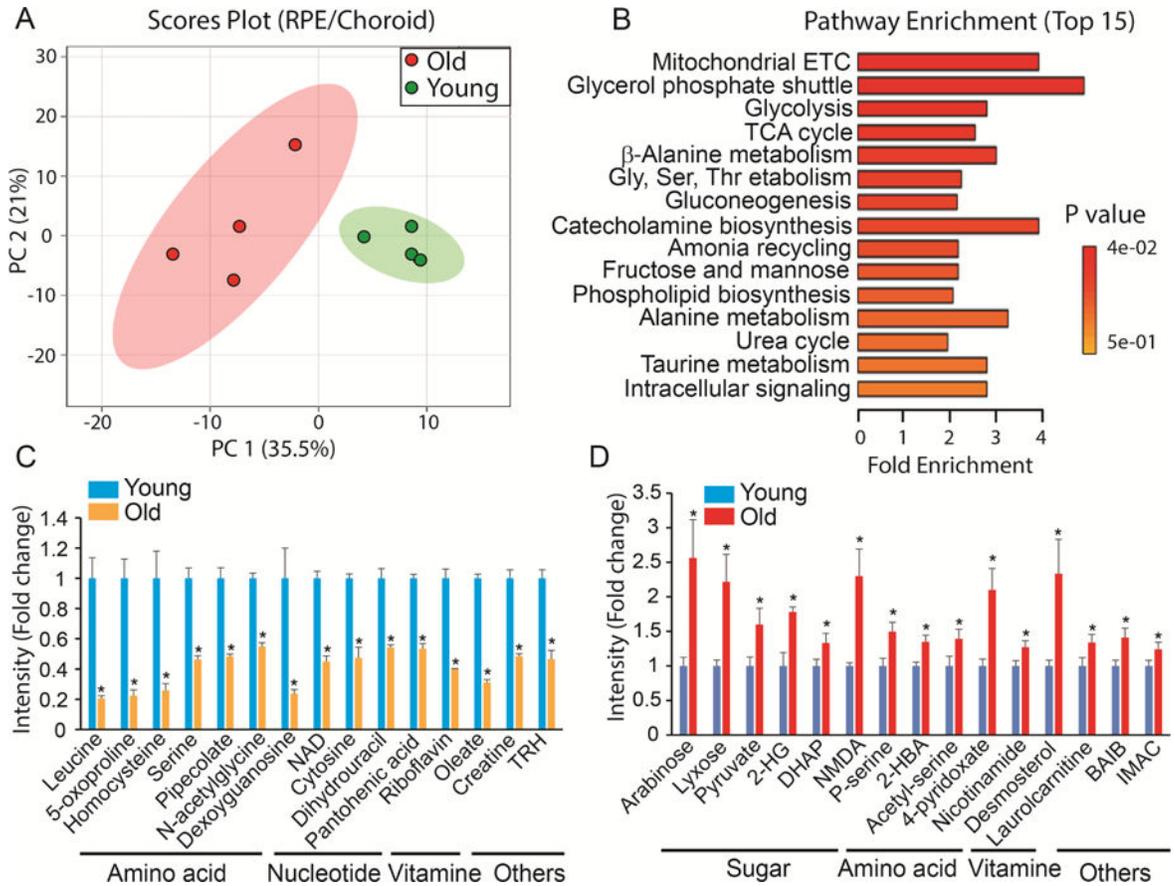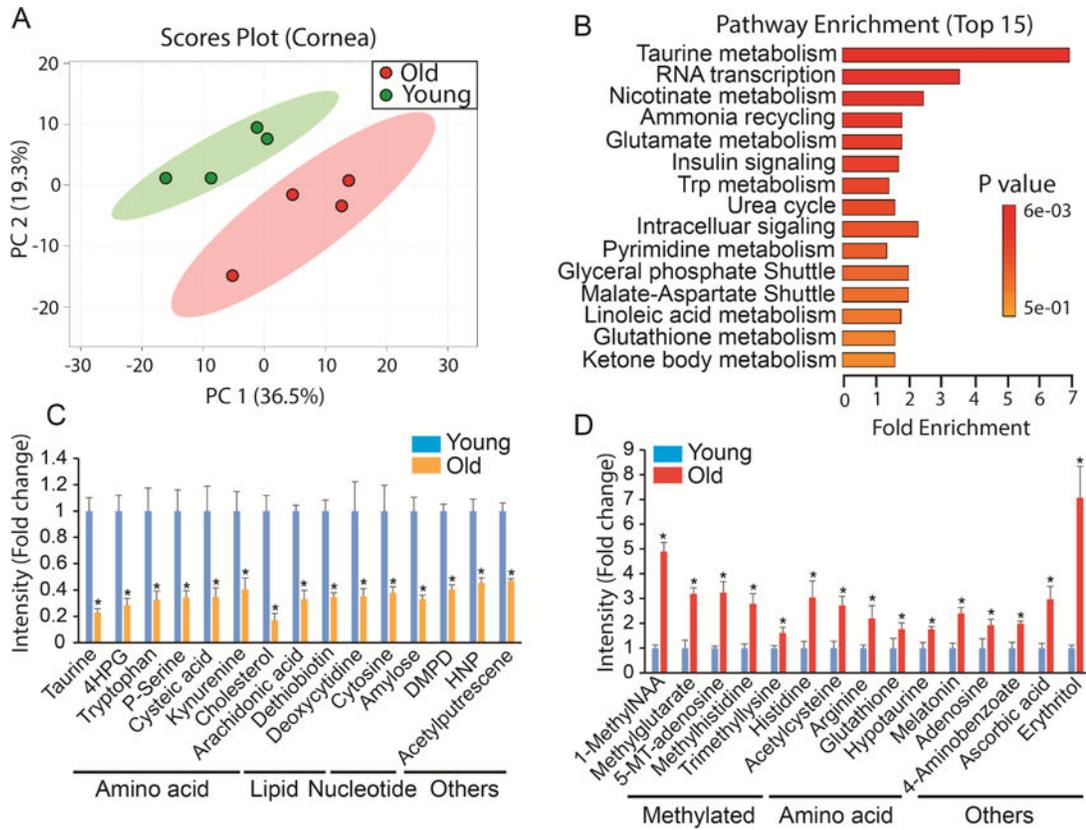
Figure 3. Differential metabolic profile between young and old RPE/choroid.
(A) Metabolites from young and old RPE/Choroid were separated into two different groups in Scores Plot by PCA. (B) Top enriched pathways from the significantly changed metabolites. (C) Top decreased metabolites in the old RPE/choroid. TRH, Thyrotropin Releasing Hormone. (D) Top increased metabolites in the old RPE/choroid. DHAP, Dihydroxyacetone Phosphate; NMDA, N-Methyl-D-Aspartic Acid; 2-HBA, 2-Hydroxybutyric Acid; BAIB, 3-Aminoisobutanoate; IMAC, 4-Imidazoleacetic Acid. Data were fold change of ion intensity of the old vs the young. N=4 from four different animals.
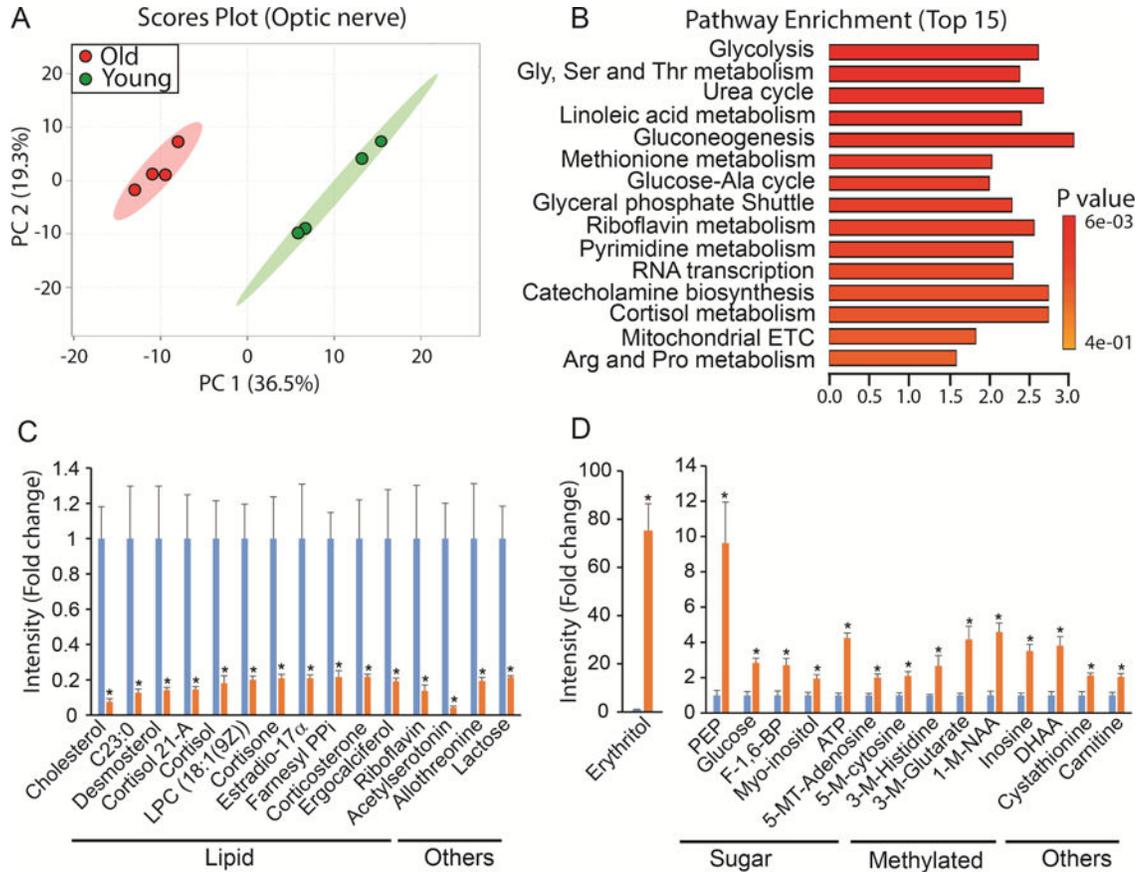
Figure 4. Differential metabolic profile between young and old lens.
(A) Metabolites from young and old lens were separated into two different groups in Scores Plot by PCA. (B) Top enriched pathways from the significantly changed metabolites. (C) Top decreased metabolites in the old lens. 5-MT-Adenosine, 5'- Methylthioadenosine; 4-GDBA, 4-Guanidinobutanoate; DMPD, N,N-Dimethyl-1,4-Phenylenediamine. (D) Top increased metabolites in the old lens. 1-methylNAA, 1-Methylnicotinamide; CDP, Cytidine 5'- Diphosphocholine. Data are fold change of ion intensity of the old vs the young. N=4.

Figure 5. Differential metabolic profile between young and old cornea.
(A) Metabolites from young and old cornea were separated into two different groups in Scores Plot by PCA. (B) Top enriched pathways from the significantly changed metabolites. (C) Top decreased metabolites in the old cornea. 4HPG, 4-Hydroxy-L-Phenylglycine; DMPD, N,N-Dimethyl-1,4-Phenylenediamine; HNP, 1-Hydroxy-2- Naphthoate. (D) Top increased metabolites in the old lens. 1-MethylNAA, 1-Methylnicotinamide; 5'-MT-Adenosine, 5'-Methylthioadenosine. Data are fold change of ion intensity of the old vs the young. N=4 from four different animals.

Figure 6. Differential metabolic profile between young and old optic nerve.
(A) Metabolites from young and old cornea were separated into two different groups in Scores Plot by PCA. (B) Top enriched pathways from the significantly changed metabolites. (C) Top decreased metabolites in the old optic nerve. Farnesyl PPi, Farnesyl pyrophosphate. (D) Top increased metabolites in the old optic nerve. 1- MethylNAA, 1-Methylnicotinamide; 5-MT-Adenosine, 5'-Methylthioadenosine; 5-M-cytosine, 5'- Methylcytosine; 3-M-Histidine, 3-methyl-L-histidine; 3-M-Glutarate, 3-methylglutarate; DHAA, dehydroascorbic acid. Data are fold change of ion intensity of the old vs the young. N=4 from four different animals.
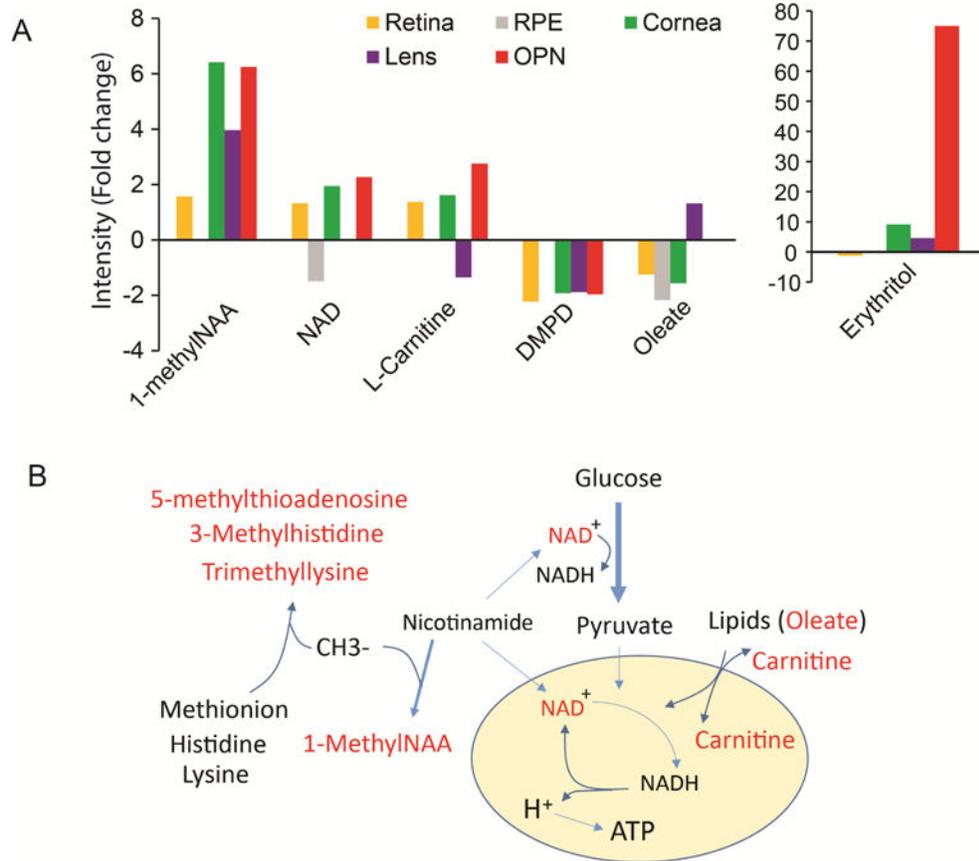
Figure 7. Common metabolic signature in the aging eye.
(A) Significantly changed metabolites at four different aging ocular tissues. 1-methylNAA, 1-Methylnicotinamide; DMPD, N,N-Dimethyl-1,4- Phenylenediamine. (B) A schematic of commonly changed metabolites in the aging eyes. The red represents the changed metabolites. Methyl group (CH3) is used by methyltransferases to methylate nicotinamide, methionine, lysine and histidine into 1-methylNAA, 5'-Methylthioadenosine, 3-methylhistidine and trimethyllysine. Nicotinamide is a precursor of NAD which is critical electron donor in both glycolysis and the TCA cycle for ATP production. Carnitine is a transporter for lipid oxidation in the mitochondria.